JOURNAL OF EXPERIMENTAL AND THEORETICAL PHYSICS, 2024, Vol. 165, No. 6, pp. 888–899

STATISTICAL, NONLINEAR, AND SOFT MATTER PHYSICS

# STUDY OF DENSE LEAD PLASMA

© 2024 E. M. Apfelbaum, A. M. Kondratyev, A. D. Rakhel*

*Joint Institute for High Temperatures of the Russian Academy of Sciences 125412, Moscow, Russia*

**e-mail: rakhel@oivtran.ru*

Received January 12, 2024
Revised January 30, 2024
Accepted January 30, 2024

**Abstract**. The thermodynamic functions and electrical resistivity of dense lead plasma were assessed at specific volumes ranging from 5 to 20 times greater than the standard value, under pressures between 0.4 and 4.0 hPa, and with specific internal energies 3 to 18 times higher than the energy required for sublimation. The recorded dependencies were later evaluated against those estimated through a classical plasma chemical model. This research aimed to uncover the effects of non-ideality on the thermodynamic characteristics and resistivity behavior of plasma. A significant finding was that the Grüneisen coefficient for this plasma varied between 0.2 and 0.4 across the entire range of states examined. Findings from the research showed that the chemical model did not accurately reflect the energy expenditure for plasma ionization and atom excitation, underestimating it by close to a factor of two, while also overestimating the temperature by a similar proportion. The inquiry additionally disclosed that in the whole spectrum of plasma states being analyzed, "pressure ionization" was a key element, and that resistivity lessened with a decrease in specific volume along isotherms.

**Keywords**: *strongly coupled plasma, Grüneisen coefficient, ionization state, the caloric properties, the sound speed, the virial theorem*

**DOI**: 10.31857/S004445102406e154

## 1. INTRODUCTION

The study of dense plasma with an ionization degree of order unity encounters serious difficulties from both theoretical and experimental perspectives. Theoretical problems are associated with the fact that for such a system, the interaction parameter, i.e., the ratio of Coulomb interaction energy between plasma particles to their kinetic energy, takes values of order unity. In this case, the application of perturbation theory using ideal gas as an unperturbed system is fairly difficult.

Experimental difficulties in studying dense plasma with developed ionization are associated with high temperatures and pressures at which such plasma can exist and which are unattainable in static experiments for the vast majority of elements in the periodic system. Various dynamic experimental methods are used to study such plasma [1–4]. However, for these experiments, questions remain open about the homogeneity of the obtained plasma and the reliable estimation of measurement uncertainties [5]. Comparison of the specific resistance values of aluminum plasma measured in experiments [4] with the results of a more accurate technique [6] showed that measurement errors [4] are 20–30% (see Fig. 7 of work [6]). The error of experiment [2] is of the same order of magnitude, as follows from the comparison presented in Fig. 5 of work [7]. Such large measurement uncertainties did not allow identifying the characteristic properties of non-ideal plasma associated with strong interaction between particles.

To study the properties of metals in liquid state and supercritical fluid state, a dynamic experimental method was developed [8], which allows measurements with accuracy not worse than 3–5 % (depending on the measured value). Using this method, measurements of thermodynamic functions and specific electrical resistance of lead [9], as well as lead-bismuth eutectic [10] were conducted for a wide range of states on the *VP*

($V$ — specific volume, $P$ — pressure). Based on the obtained data, caloric equations of state (EOS) of these fluids were constructed and critical points of liquid-gas transition and metal-nonmetal transition were estimated [10]. A significant feature of such EOS is that its accuracy depends only on the error of experimental data, based on which two characteristic functions are determined: the dependence of the Grüneisen coefficient and the cold component of internal energy on specific volume. Since in each individual experiment [9, 10] the dependence of specific internal energy of the sample on specific volume and pressure is measured along some line on the $VP$-plane (which extends from the normal state), rather than at a single point on the shock adiabat or unloading isentrope, as is the case in shock-wave experiments [11], this allows for sufficiently accurate analysis of isochore behavior in the *PE -plane* ($E$ — specific internal energy). Based on such analysis, a general pattern was established: within measurement error, these isochores are straight lines. This fact made it possible to establish the form of function *P(V, E)*, i.e., the caloric EOS, based on general thermodynamic relations [12], and also to measure with necessary accuracy the dependencies of the Grüneisen coefficient and cold component of internal energy on relative volume [9,10]. This eliminates the need to make assumptions about the form of these dependencies [11].

Measurement errors [9, 10] for the range of specific volumes close to the normal value, for which accurate literature data is available, were reliably estimated and proved to be no worse than 3 %. However, for the region of states $P > 0.3$ hPa, $V > 4V_0$ ($V_0$ — normal value of specific volume of the studied metal) there is no literature data. To estimate the systematic error of experiments in this region of states, a method was developed for direct measurement of shock wave velocities excited in the sample during the dynamic experiment. Since the shock adiabat of the studied metal can be determined using a pre-constructed caloric EOS, and the accuracy of the latter, as noted above, depends only on the accuracy of experimental data, then by comparing the measured shock wave velocities with values calculated using EOS, it is possible to estimate the systematic measurement error at large values of sample specific volume and pressure. Such work was performed in experiments with lead [13], and measurement errors were estimated for the volume range $V/V_0 = 2 - 7$ and pressure range $P = 0.4 - 3.4$ hPa. In this work, experimental data on the properties of dense lead plasma for the region of states $V/V_0 = 6 - 20$, $P = 0.4 - 4$ hPa are presented.

To interpret the results of these experiments, a chemical plasma model (CPM) [14,15] was used. In this model, plasma is considered as an equilibrium mixture of neutral atoms, positive ions with charges $ze = 1–4$ ($e$ — elementary charge, $z$ — ionization degree) and electrons. The free energy of plasma is represented as the sum of the free energy of an ideal gas of such particles and three terms that describe three types of interactions between them: interaction between charged particles, between charged particles and atoms, and interaction between atoms. Note that ions in this model are considered as point-like classical particles, and the contribution to free energy from interactions between ions, as well as between ions and free electrons, is described using an analytical dependence [16]. Charge-atom and atom-atom interactions are described considering only pair interactions, i.e., up to the second term of the virial expansion. Minimization of free energy with respect to the numbers of particles of all types allows determining the plasma composition (at given values of temperature, volume, and total number of atoms). After calculating the plasma composition, its thermodynamic functions can be determined, which are obtained by differentiating free energy as a function of specific volume and temperature. The resistivity of plasma was calculated within the relaxation time approximation [14]. Since the CPM used here has already been described in detail [14,15], we will not discuss it here. We only note that, strictly speaking, this model can be applied to describe relatively low-density plasma, when it is possible to determine with sufficient accuracy such composite particles as molecules, isolated atoms, or ions. However, despite the limited range of applicability, chemical plasma models allow obtaining qualitatively correct results even for the region of states where the interaction parameter is not small [17, 18].

In this work, measurements of thermodynamic functions and specific resistance of lead were carried out for the region of states where specific volume, temperature, and pressure exceed the values at the critical point of the liquid-gas phase transition. As known, the states of matter where temperature and pressure exceed critical values is called a supercritical

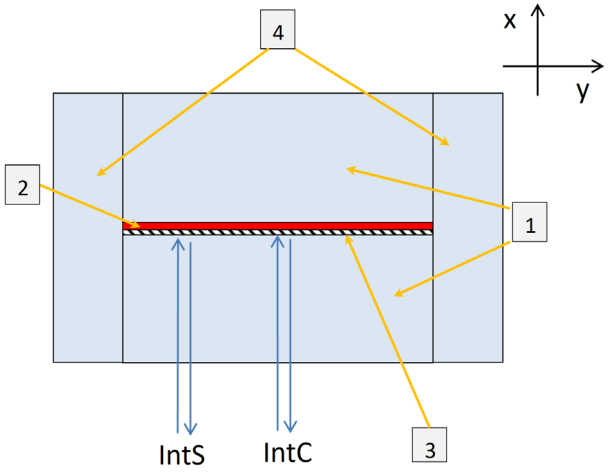


**Fig. 1.** Cross-sectional diagram of the experimental assembly by a plane perpendicular to the electric current direction: window material plates (*1*); sample (*2*); side plates of technical glass (*4*). The direction of the two laser interferometer beams (IntC, IntS) is shown, as well as the dielectric mirror (*3*) from which the interferometer beams are reflected (mirror is applied to the plate surface)

fluid. In this work, consequently, we will deal with gaseous supercritical fluid. Such fluid, as will be shown below, has relatively low resistivity: its values are only 2–6 times higher than the specific resistivity of liquid lead in metallic state near the Mott-Ioffe-Regel limit [9]. Thus, there is good reason to call such supercritical fluid a dense plasma. The main goal of this work was to discover characteristic features of dense plasma (in thermodynamic functions and specific resistance behavior) related to strong interaction between particles.

In case of classical plasma, where electron degeneracy and quantum scattering effects are insignificant, the interaction parameter is usually taken as the ratio of potential energy of electrostatic repulsion between neighboring ions located at average distance from each other (without considering correlations) to their average kinetic energy. If we denote the average number of ions per unit volume as $n_j$, then the average distance between them will be of order $n_i^{-1/3}$, and their average kinetic energy, according to equipartition law, will be of order of temperature. For the coupling parameter, which we will denote by Γ, we get the expression

$$\Gamma = \frac{z^2 e^2}{kT} n_i^{1/3}, \qquad (1)$$

where $T$ is temperature, $k$ is Boltzmann constant. For lead plasma studied in this work, $nj = (1 - 8) \cdot 10^{21}$ cm$^{-3}$, $T = 10 - 40$ kK, $z = 1 - 2$, $\Gamma = 0.5 - 5$. In this case, the ionic component of plasma is not degenerate, and the degeneracy parameter of the electronic component $\vartheta = kT / \varepsilon_F$ takes values $\vartheta = 1 - 10$, where $\varepsilon_F$ is Fermi energy, which is determined according to formula

$$\varepsilon_F = \frac{n^2}{2m}\left(3\pi^2 n_e\right)^{2/3}, \qquad (2)$$

where $m$ is electron mass, $n_e$ is average number of electrons per unit volume.

## 2. DESCRIPTION OF THE EXPERIMENTAL TECHNIQUE

For measurements, the experimental technique developed in works [9,10] was used. Let us note only some changes that were introduced during the execution of this work. After the systematic error of such measurements was evaluated at large values of specific volume of the sample [13], it became possible to study the properties of metals in gaseous state. Lead was chosen as the sample material for studying dense plasma because samples of required thickness and quality for our experiments (foil strips) could be manufactured in the laboratory. In this case, the foils had to be made sufficiently thin (9–15 μm). This is necessary to maintain uniform heating of the sample and its one-dimensional thermal expansion even at large volume values. This requires meeting two conditions: the sample thickness should be small compared to its width and length (which were about 10 mm for these experiments), and the substance velocity should be small compared to the speed of sound. Since the measurement time for such experiments is about 1 μs and is actually determined by the geometric dimensions of the window plates, obtaining large thickness increments of the sample during this time, at relatively low velocities, imposes an upper limit on its initial thickness. Lead was also chosen because experimental data on the properties in the liquid state had been previously obtained [9, 13], and this allowed for a more accurate assessment of the errors in the present measurements.

To control the one-dimensionality of the sample's thermal expansion at high volume values, two interferometers were used simultaneously

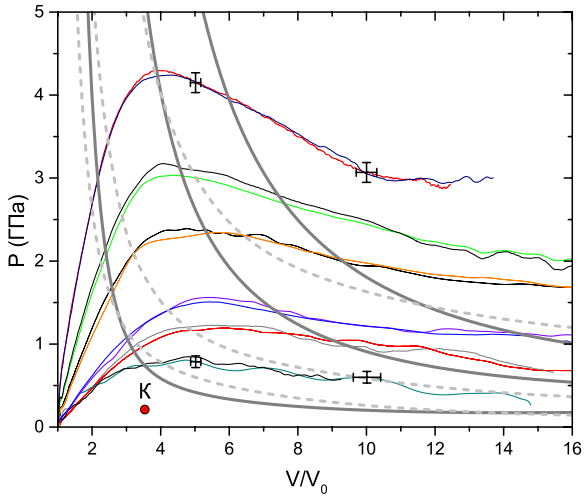


**Fig. 2.** State region on the *VP*-plane, for which measurements of thermodynamic functions and specific resistance of lead fluid were performed. The family of lines emerging from the normal state represents quasistatic processes under which measurements were conducted. The critical point (*K*) and isentropes (three thick solid gray lines) were obtained using EOS from work [13]. Dashed gray lines are isotherms T = 20, 30, 50 kK, EOS from work [11]. Crosses show measurement uncertainties

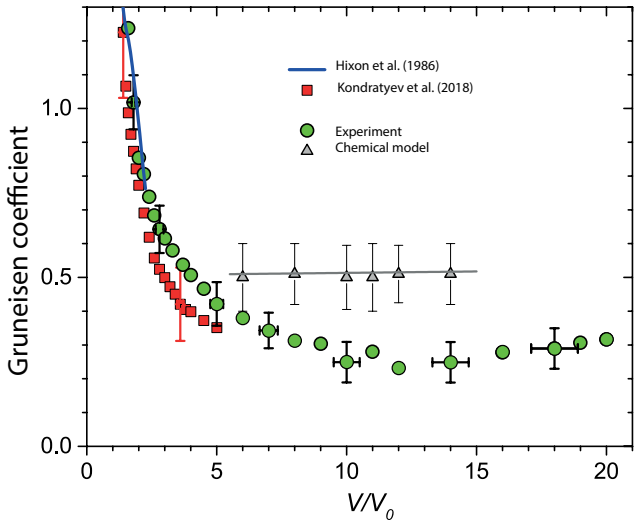


**Fig. 3.** Grüneisen coefficient of lead fluid as a function of relative volume. The experimental data obtained in this work (green circles) are compared with measurement results from works [9] (red squares) and [19] (blue line), as well as with calculations using SHM (gray triangles and the straight line approximating these values). For experiments, crosses indicate measurement errors, and for the model - the range of Grüneisen coefficient variation for a specific relative volume value

in the present experiments. The cross-sectional diagram of the sample and the interferometer arrangement are shown in Fig. 1. The beam of one interferometer (IntC) was reflected from the central part of the sample surface, while the spot of the second interferometer (IntS) was shifted sideways by 2–3 In these experiments, two window plates with dimensions of $5\times10\times10$ mm$^3$ were used. The glued experimental assembly, consisting of two window plates, sample, and side plates of technical glass, represented a rectangular parallelepiped with two edges having a length of about 10 mm, and the third one (which is parallel to the axis in Fig. 1) – 16 mm. In all experiments, the width and length of the sample were equal to the width and length of the 10 mm, window plates, respectively. Such assembly allowed maintaining practically one-dimensional deformation of the window material plates during time $t \leq 2D / c_l$, where $D$ — is the plate thickness, and $c_l$ — is the longitudinal sound velocity in the window material. The present experiments showed that the relative difference between the sample surface displacements easured by the two interferometers did not exceed 2% up to the maximum sample volume values.

The region of states on the *VP*-plane, for which measurements of thermodynamic functions and resistivity of supercritical lead fluid were performed, is shown in Fig. 2. Previously, it was discovered that when liquid lead is heated under pressure of 0.5-4 hPa, it undergoes a metal-nonmetal transition near the relative volume value $V/V_0 \approx 4$, which practically coincides with the critical volume value of the liquid-gas transition [10, 13]. This critical point is marked in Fig. 2. As shown in the figure, for supercritical volume values, measurements were conducted at supercritical pressures and, consequently, at supercritical temperatures. It is also evident that the state region studied in this work is significantly expanded compared to work [9], which obtained data for the volume interval $V/V_0 \leqslant 5$. To characterize in more detail the quasi-static processes under which measurements were conducted in present experiments, Fig. 2 shows three isentropes, obtained using EOS from work [13]. For this EOS, characteristic functions were determined based on the entire set of experimental data for lead, including data from this work. Fig. 2 also shows three isotherms of the interpolation EOS [11]. As shown in the figure, in the region of supercritical volumes for experiments with pressure

$P < 1$ hPa, these processes are close to isothermal, and for experiments with pressure $P > 1$ hPa — to isobaric.

## 3. MEASUREMENT RESULTS

Figure 3 shows the measurement results obtained in this work for the dependence of the Grüneisen coefficient on relative volume. These re sults are compared with experimental data from works [9] and [19], as well as with results obtained by the CPM. The Grüneisen coefficient, which we denote as $\Upsilon$, is defined by the formula

$$\gamma = \left(\frac{\partial PV}{\partial E}\right)_V. \tag{3}$$

The value of the Grüneisen coefficient for a certain specific volume was determined by the method of least squares of the data points *PV, E*, obtained for this volume in all experiments of the present work. It was verified that specifically linear approximation (rather than a higher-degree polynomial) is the most accurate.

From Figure 3, it follows that in the volume range $V/V_0 = 6 - 14$ our model predicts an almost constant value of the Grüneisen coefficient, being close to the value 2/3, which this coefficient takes for a monatomic ideal gas of constant composition. However, the values calculated using chemical model (which were determined for the same ranges of energy and pressure values as in the experiment) in the interval $V/V_0 = 10 - 14$ are almost twice the measured values. As seen in Figure 3, the difference between calculated and measured values is minimal at volumes $V/V_0 = 5 - 6$, for which our chemical model is, strictly speaking, not applicable.

The decrease in the Grüneisen coefficient to values less than 2/3 can be explained by the presence of strong interaction between charged plasma particles and ionization (composition change). Let us show that for plasma with strong Coulomb interaction, the inequality $\gamma < 2/3$ must be satisfied. For simplicity, we will assume that the plasma is fully ionized. Using the expression for the free energy of weakly non-ideal classical plasma [20], we find

$$\gamma = \frac{2}{3} - \frac{\sqrt{2\pi}}{9}\Gamma^{3/2}, \tag{4}$$

from which it follows that in this case, the inequality $\gamma < 2/3$ is indeed satisfied. This formula is derived for weakly non-ideal plasma ($\Gamma \leqslant 1$), but if we use it to estimate the Grüneisen coefficient at values $\Gamma \approx 1$, we obtain values $\gamma \approx 0.3$. Therefore, we can expect that strong electrostatic interaction between plasma particles leads to a decrease in the Grüneisen coefficient to the observed values.

Let us now show that for plasma in which ionization occurs, the Grüneisen coefficient also becomes less than 2/3. For simplicity, let's consider ideal plasma at temperatures where only single ionization of atoms occurs. In this case, the formulas for pressure and specific internal energy of plasma will take a relatively simple form:

$$PV = \frac{R}{A}\left[1 + \alpha(T)\right]T, \tag{5}$$

$$E = \frac{3}{2}PV + \frac{N_A}{A}I_1\alpha(T), \tag{6}$$

where $R$ is the gas constant, $A$ is the molar mass of gas, $N_A$ is Avogadro's number, $I_1$ is the first ionization potential, $\alpha$ — the degree of gas ionization. The degree of ionization is determined according to the relation $\alpha = n_e/n_n$, where $n_n$ is the total number of atoms per unit volume (i.e., the sum of ionized and neutral atoms). Substituting expressions (5), (6) into formula (3), for the Grüneisen coefficient we obtain

$$\gamma = \left[\frac{3}{2} + \frac{\frac{I_1}{k}\left(\frac{\partial\alpha}{\partial T}\right)_V}{\left(\frac{\partial\alpha}{\partial T}\right)_V + \alpha + 1}\right]^{-1}. \tag{7}$$

Since the degree of ionization increases with temperature at constant volume, the second term in brackets is always positive, and consequently, $\Upsilon < 2/3$. It should be noted that in deriving formula (7), we neglected the energy contribution from atomic excitations, assuming that ionization occurs from the ground state of the atom. However, if such contribution is considered, it is obvious in advance that it will also lead to a decrease in the Grüneisen coefficient.

Thus, the fact that our measured values of the Grüneisen coefficient are significantly lower than may indicate both strong interaction between lead

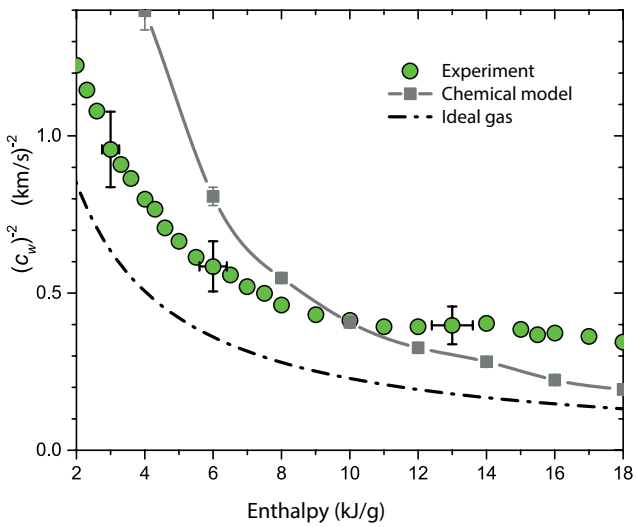


**Fig. 4.** Isenthalpic compressibility of supercritical lead fluid as a function of specific enthalpy. Green circles – experiment, solid gray line with markers – CPM, dash-dotted black line – dependence calculated for ideal gas. For experiments, crosses indicate measurement errors, and for the model – the range of isenthalpic compressibility variation at a certain enthalpy value

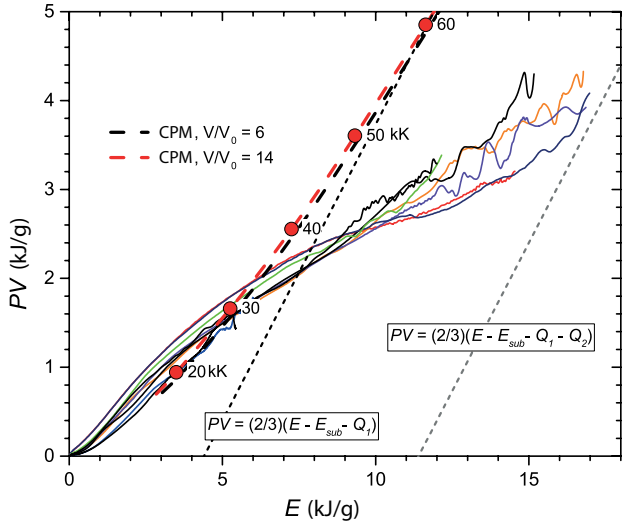


**Fig. 5.** Measured dependencies of $PV$ on $E$ (thin solid lines starting from the origin) are compared with dependencies calculated using CPM for two isochores (thick black and red dashed lines), red circles indicate calculated temperature values (in kK) on the isochore $V/V_0 = 14$. Thin dashed lines show dependencies for singly ($\alpha = 1$) and doubly ($\alpha = 2$) ionized ideal lead gas of constant composition

plasma particles and the process of developed ionization. Since accurate calculation of the ionization degree of such plasma requires correct description of the particle interaction influence on ionization potential reduction, shifts in atomic electron levels, and electron transition probabilities between atoms, this problem cannot be solved within the CPM framework. The interpretation of the dense plasma Grüneisen coefficient behavior observed here, which follows from very general considerations, will be given in the next section.

Let us consider another thermodynamic quantity that is directly determined from the results of present experiments and characterizes mechanical properties of plasma. This refers to the partial derivative of density with respect to pressure at constant enthalpy: $(\partial\rho/\partial P)_W$, where $\rho = V^{-1}$ is density, and the letter $W$ will denote specific enthalpy. This derivative, which we will call isenthalpic compressibility, is conveniently expressed through the isenthalpic sound velocity $c_w$, which we define according to the formula

$$c_w^{\,2} = \left(\frac{\partial P}{\partial \rho}\right)_W. \qquad (8)$$

The usual sound velocity $c_s$ (isentropic) is related to $c_w$ by the relation

$$c_s = (\gamma + 1)^{1/2} c_w. \qquad (9)$$

Figure 4 shows the dependence of isenthalpic compressibility of supercritical lead fluid on specific enthalpy. As seen in Fig. 4, within measurement uncertainty, this quantity is a function of a single variable – enthalpy and, consequently, practically does not depend on pressure. The values calculated using CPM also fall well on a single line. However, the compressibility values obtained using the model differ significantly from measurement results: at low enthalpy values, these values are almost twice higher than measured values, and at enthalpy values of 16–18 kJ/g, they are almost twice lower. Note that in the range $W > 14$ kJ/g, the calculated compressibility values are close to those for ideal gas (where gas enthalpy is measured from the normal state of solid body).

The fact that CPM predicts significantly higher compressibility at low enthalpy values, which correspond to low specific volumes for these experiments, can be explained by the fact that in this model, ions are point-like and repulsion associated with their finite size is absent. Note that the enthalpy value of 5 kJ/g was achieved in these experiments at volumes $V/V_0 = 4$–8. The relatively low values of isenthalpic compressibility predicted by CPM at high enthalpy values are explained by

**Table 1.** Measured values in this work of pressure $P$ (hPa), specific internal energy $E$ (kJ/g) and specific resistance $\sigma^{-1}$ (μΩ•m) of supercritical lead fluid on isochores $V/V_0$ = 5, 6, 8, 10, 12, 14, 18

| $V/V_0$ | $P$ | $E$ | $\sigma^{-1}$ | $V/V_0$ | $P$ | $E$ | $\sigma^{-1}$ |
|---|---|---|---|---|---|---|---|
| 5 | 4.16 | 5.44 | 15.43 | 10 | 3.05 | 11.55 | 15.01 |
| 5 | 4.16 | 5.42 | 15.38 | 10 | 3.07 | 11.37 | 15.07 |
| 5 | 3.00 | 3.84 | 20.56 | 10 | 2.44 | 7.23 | 19.06 |
| 5 | 2.32 | 3.33 | 23.50 | 10 | 1.98 | 6.13 | 21.61 |
| 5 | 2.45 | 3.18 | 24.28 | 10 | 1.98 | 6.00 | 22.29 |
| 5 | 2.39 | 3.34 | 23.47 | 10 | 1.98 | 6.01 | 22.31 |
| 5 | 2.37 | 3.20 | 23.92 | 10 | 1.93 | 5.88 | 21.82 |
| 5 | 1.49 | 2.48 | 32.15 | 10 | 1.93 | 5.69 | 23.19 |
| 5 | 1.38 | 2.54 | 31.04 | 10 | 1.22 | 3.98 | 37.67 |
| 5 | 2.36 | 3.28 | 23.78 | 10 | 1.21 | 3.96 | 37.06 |
| 5 | 1.16 | 2.06 | 33.78 | 10 | 1.03 | 3.40 | 50.37 |
| 5 | 1.08 | 2.08 | 37.22 | 10 | 0.91 | 3.04 | 58.98 |
| 5 | 1.21 | 2.16 | 36.17 | 10 | 0.96 | 3.26 | 52.91 |
| 5 | 1.25 | 2.15 | 35.95 | 10 | 1.00 | 3.24 | 50.47 |
| 5 | 0.79 | 1.84 | 44.66 | 10 | 0.60 | 2.33 | 97.96 |
| 5 | 0.84 | 1.90 | 41.71 | 12 | 2.97 | 14.22 | 15.02 |
| 5 | 0.82 | 1.70 | 42.32 | 12 | 2.92 | 13.95 | 15.06 |
| 6 | 3.94 | 6.65 | 15.40 | 12 | 2.23 | 8.48 | 18.63 |
| 6 | 3.98 | 6.59 | 15.36 | 12 | 1.83 | 7.12 | 20.79 |
| 6 | 2.91 | 4.61 | 20.43 | 12 | 1.85 | 6.98 | 21.49 |
| 6 | 2.34 | 4.00 | 23.72 | 12 | 1.85 | 6.93 | 21.25 |
| 6 | 2.36 | 3.83 | 24.79 | 12 | 1.79 | 6.81 | 21.10 |
| 6 | 2.34 | 3.96 | 23.85 | 12 | 1.79 | 6.45 | 22.34 |
| 6 | 2.32 | 3.85 | 23.89 | 12 | 1.12 | 4.42 | 35.55 |
| 6 | 2.28 | 3.87 | 24.18 | 12 | 1.14 | 4.38 | 36.34 |
| 6 | 1.49 | 2.86 | 35.40 | 12 | 0.92 | 3.69 | 51.47 |
| 6 | 1.40 | 2.90 | 34.35 | 12 | 0.80 | 3.18 | 62.81 |
| 6 | 1.19 | 2.40 | 41.20 | 12 | 0.94 | 3.38 | 57.21 |
| 6 | 1.09 | 2.38 | 44.45 | 12 | 0.79 | 3.51 | 51.29 |
| 6 | 1.22 | 2.51 | 42.25 | 12 | 0.39 | 2.41 | 114.37 |
| 6 | 1.21 | 2.49 | 41.59 | 14 | 2.17 | 9.91 | 18.55 |
| 6 | 0.68 | 2.02 | 56.85 | 14 | 2.13 | 9.75 | 18.47 |
| 6 | 0.76 | 2.07 | 53.91 | 14 | 1.78 | 8.08 | 20.21 |
| | 0.75 | 1.86 | 56.64 | 14 | 1.75 | 7.95 | 20.81 |

**Table 1. (Contd.)**

| $V/V_0$ | $P$ | $E$ | $\sigma^{-1}$ | $V/V_0$ | $P$ | $E$ | $\sigma^{-1}$ |
|---|---|---|---|---|---|---|---|
| 8 | 3.54 | 8.99 | 15.18 | 14 | 1.74 | 7.84 | 21.03 |
| 8 | 3.50 | 8.88 | 15.22 | 14 | 1.72 | 7.73 | 20.54 |
| 8 | 2.65 | 5.97 | 19.65 | 14 | 1.73 | 7.15 | 21.95 |
| 8 | 2.15 | 5.12 | 22.77 | 14 | 1.11 | 4.81 | 34.51 |
| 8 | 2.13 | 4.97 | 23.53 | 14 | 1.13 | 4.73 | 35.60 |
| 8 | 2.13 | 5.04 | 23.39 | 14 | 0.74 | 3.99 | 50.57 |
| 8 | 2.17 | 4.90 | 22.83 | 14 | 0.67 | 3.27 | 65.90 |
| 8 | 2.10 | 4.86 | 23.31 | 14 | 0.79 | 3.48 | 59.63 |
| 8 | 1.33 | 3.47 | 37.17 | 14 | 0.40 | 2.48 | 129.89 |
| 8 | 1.32 | 3.49 | 36.78 | 18 | 2.14 | 12.16 | 18.45 |
| 8 | 1.11 | 2.97 | 48.15 | 18 | 1.67 | 10.02 | 19.56 |
| 8 | 0.98 | 2.78 | 53.68 | 18 | 1.60 | 9.90 | 20.12 |
| 8 | 1.07 | 2.96 | 49.35 | 18 | 1.64 | 9.67 | 20.00 |
| 8 | 1.16 | 2.99 | 46.80 | 18 | 1.67 | 9.39 | 20.28 |
| 8 | 0.63 | 2.21 | 78.17 | 18 | 1.02 | 5.49 | 32.82 |
| 8 | 0.63 | 2.29 | 75.48 | 18 | 1.06 | 5.29 | 34.74 |
| 8 | 0.70 | 2.06 | 82.64 | 18 | 0.55 | 4.36 | 50.63 |

the fact that, as will be shown below, this model overestimates plasma temperature by almost a factor of two.

For a more detailed comparison of measurement results with CPM predictions, Fig. 5 shows the dependencies of $PV$ on specific internal energy $E$. To avoid cluttering the figure, results are shown for a small group of experiments in which maximum values of specific volume and internal energy were achieved. In Fig. 5, it can be seen that significant deviation of calculated dependencies from measured ones begins at energy values of 6–7 kJ/g. At higher energy values, the calculated dependencies become close to the dependency for singly ionized ideal gas. For reference, the specific ionization energy values for single, double, and triple ionization of ideal lead gas atoms are: $Q_1$ = 3.44 kJ/g, $Q_2$ = 6.97 kJ/g and $Q_3$ = 14.8 kJ/g [21]. Using the sublimation energy value for lead $E_{sub}$ = 0.942 kJ/g [22], for internal energy of singly ionized ideal lead gas at temperature

$T = 10 - 30$ kK, we obtain energy values of $E = 6 - 8$ kJ/g. This estimate shows that calculated dependencies begin to deviate from measured ones when double ionization of atoms begins, and it might seem that the ionization degree predicted by the model does not exceed one. However, this is not the case.

The degree of ionization as a function of plasma specific internal energy, calculated using CPM for isochores $V/V_0 = 6$, $V/V_0 = 14$, is shown in Fig. 6. It can be seen that it increases monotonically and reaches a value of 1.9. The figure also shows the dependence of the value $E-(3/2)PV$ on plasma internal energy values. For classical plasma, this value equals the energy that goes into ionization, since the value $(3/2)PV$ is the average kinetic energy of a classical particle system. As follows from Fig. 6, in the energy range $E-(3/2)PV$ kJ/g, the calculated values of are about 5 kJ/g, which is two times less than the measured values. Thus, CPM predicts almost two times lower energy expenditure for plasma ionization compared to the values obtained in the experiment. This implies that the plasma temperature values predicted by this model may be significantly overestimated.

For detecting plasma non-ideality effects, studying the behavior of electrical conductivity is very important [17,18]. Fig. 7 shows the measured dependence of lead fluid's resistivity on specific internal energy in this work. Also presented are the resistivity dependencies on isochores obtained from these experimental data. The figure clearly shows the characteristic behavior of isochores near the metal-nonmetal transition [10]. This transition manifests in that near the volume value $V/V_0 = 2.7$ the temperature coefficient of resistance changes sign from positive to negative and the metal transitions into a strongly correlated metallic state. When specific volume becomes larger than value $V/V_0 \approx 4$, this coefficient, being negative, begins to rapidly increase in absolute magnitude with volume increase. The critical density estimation for metal-nonmetal transition in supercritical lead fluid was made based on analysis of the "cold curve", i.e., temperature-independent part of internal energy [10]. As follows from Fig. 7, in plasma state ($V/V_0 > 4$) the resistivity on isochores monotonically decreases with energy increase. It is noteworthy that the dependencies calculated using CPM in the energy interval $E < 5$ kJ/g practically merge into

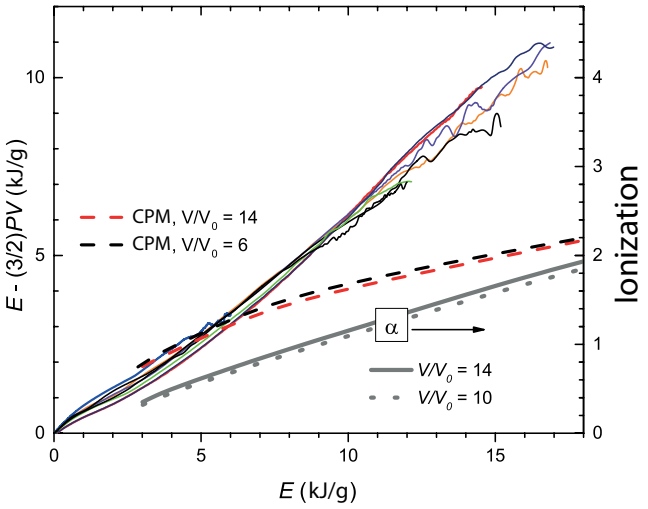


**Fig. 6.** The measured dependencies of the value $E-(3/2)PV$ on specific internal energy (thin lines originating from the origin) are compared with dependencies calculated using CPM for two isochores (two thick dashed lines). The plasma ionization degree dependencies calculated using CPM for two isochores are shown by gray solid and gray dotted lines

one line, which is not observed experimentally. Also note that at energy values $E > 10$ kJ/g, the slopes of measured isochores are significantly less than those demonstrated by the model. Experimental isochores of resistivity in this energy interval become almost horizontal. With increasing relative volume, agreement between measured dependencies and calculated ones improves. Note that calculation of lead plasma resistivity for volumes $V/V_0 = 10 - 20$ on isotherm $T = 20$ kK [23] gives resistivityvalues in the interval 50–100 μOhm, which agree with our calculation results.

The results of our measurements of pressure, specific internal energy, and resistivity of supercritical lead fluid for a family of seven isochores are presented in Table 1.

## 4. DISCUSSION OF THE OBTAINED RESULTS

As follows from Fig. 5, our chemical model predicts rather high plasma temperature values. Due to such high temperatures, a question arises about the estimation of measurement errors in the present study related to energy losses through thermal radiation. For lead plasma with density of 0.5–2.0 g/cm$^3$ at temperature of 1-5 eV, the mean free path of photons (Rosseland averaged) is ~ $10^{-6}$ cm [24, 25], which is much smaller than the plasma

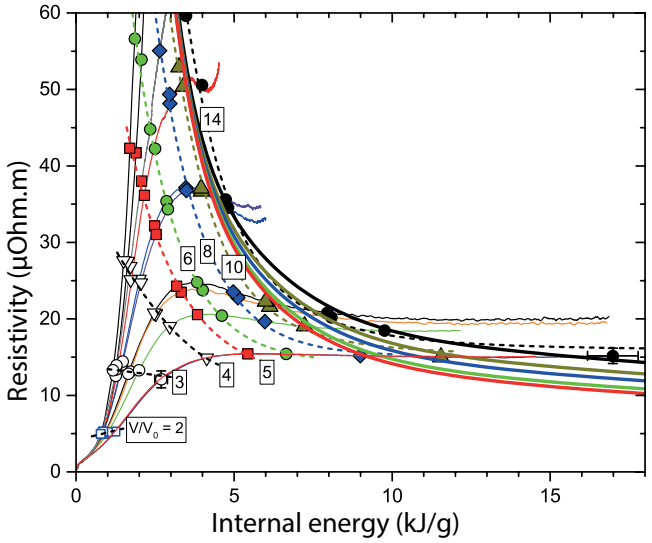


**Fig. 7.** Specific resistance of lead as a function of specific internal energy. Thin solid lines emerging from the normal state are dependencies measured in experiments of this work (marked with the same colors as these experiment lines in Fig. 2), symbols are specific resistance values on isochores obtained in these experiments, thin dotted lines are approximations of these isochores, thick solid lines are isochores $V/V_0 = 5, 6, 8, 10, 14$, calculated using CPM (marked with the same colors as corresponding experimental isochores)

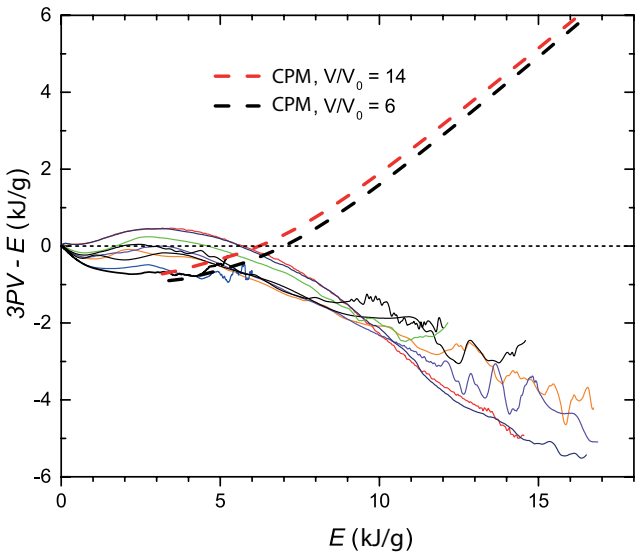


**Fig. 8.** Change in the average kinetic energy of lead fluid relative to the normal state as a function of internal energy. Thin solid lines originating from the origin are dependencies measured in present experiments, two thick dashed lines are dependencies calculated using CPM for two isochores

sample thickness in our experiments. This implies that this plasma is opaque and thermal radiation emerges from a thin layer near the sample surface. If we estimate the radiation losses from above, assuming that the sample temperature increases as predicted by the model, and its surface radiates as a black body, and all radiation energy is lost by the sample, it turns out that even for experiments with maximum pressure values, these losses do not exceed 10 % of the sample energy up to the energy value of 10 kJ/g. However, as seen in Fig. 6, at this energy value, the difference between measured and calculated values of $PV$ reaches 50% and, consequently, this difference cannot be explained by energy losses through thermal radiation.

It should also be noted that the present experiments were conducted with samples whose initial thickness varied by almost 3 times in different experiments, and sapphire and silica glass were used as window materials, whose optical properties differ significantly from each other, and therefore energy losses due to radiation in different experiments, if they were noticeable, would have been different. However, the data obtained in various experiments are in good agreement with each other. Furthermore, measurements of sample volume and pressure, whose accuracy is not affected by thermal radiation, demonstrate rather smooth and monotonic pressure-volume dependencies, which approach practically constant pressure values at large sample volumes. If thermal radiation losses were significant, then due to the sharp dependence of thermal radiation intensity on temperature, one could expect a more or less sharp decrease in pressure in the sample.

Thus, our CPM predicts significantly lower energy expenditure for ionization and excitation of atoms than the values obtained in the experiment. This suggests that the model overestimates plasma temperature (for given values of $V$ and $E$). As shown in Fig. 5, at an energy value of 12 kJ/g, the calculated values of $PV$ are approximately 1.7 times higher than the measured ones. If we assume that the kinetic energy of plasma particles, which is proportional to $(1 + \alpha)\ T$, is overestimated by the same factor, and considering that the ionization degree in our model is practically independent of density and increases almost linearly with temperature (see Fig. 6), then instead of the temperature value of 60 kK predicted by the model, we get 40 kK. If we reduce the plasma temperature values by 1.7 times (relative to the values given by the model), then the maximum energy losses due to radiation will not exceed up to the 5% maximum measured energy values. Certainly, this temperature estimate cannot claim high accuracy,

but it agrees with the results of present experiments, which showed no significant energy losses.

There is another experimental confirmation of the correctness of this conclusion. As follows from Fig. 4, in the enthalpy range of $W > 8$ kJ/g (which corresponds to the energy range of $E > 6$ kJ/g), the dependence of isenthalpic compressibility on specific enthalpy becomes very flat. On the other hand, radiation energy losses cannot affect this dependence since they do not influence density and pressure measurements, and compressibility is practically independent of enthalpy. Since the calculated compressibility values for this enthalpy range become almost twice lower than the measured ones, this definitely indicates that the model gives overestimated temperature values by approximately two times. Note that the temperature values obtained using the interpolation EOS [11] also turn out to be overestimated.

Due to such a significant difference between experimental results and XMP predictions, let's try to interpret these results based on general considerations that are not tied to any particular model. For this, we will use the virial theorem, which establishes the relationship between the average kinetic energy of a system of particles interacting according to Coulomb's law, with internal energy and pressure [20]:

$$K = 3PV - E, \tag{10}$$

where $K$ is the average kinetic energy of the system. Note that this theorem is valid for both classical and quantum particle systems. For a classical particle system $K = (3/2)NkT$ ($N$ is the number of particles in the system). Substituting this expression into (10) and differentiating it with respect to $E$ at fixed volume and number of particles $N$, we obtain

$$\gamma = \frac{1}{3} + \frac{k}{2c_v}, \tag{11}$$

where $c_v$ is the heat capacity per particle. From this, it follows that for classical plasma of constant composition, the following inequalities hold $1/3 < \gamma \leqslant 2/3$. We emphasize that this result is no longer restricted by the assumption of weak coupling that was used in deriving formula (4).

Let's consider the case when the number of particles in the system changes due to ionization. We will examine plasma consisting of atoms, ions, and free electrons at temperatures where only single ionization of atoms occurs. The kinetic energy of such a particle system consists not only of the kinetic energy of "classical particles" listed above but also of “quantum” particles of bound electrons in atoms. Differentiating relation (10) with respect to energy at fixed volume, we obtain

$$\left(\partial K / \partial E\right)_V = 3\gamma - 1. \tag{12}$$

Consider that the increment of kinetic energy is related not only to the increase in kinetic energy of “classical” particles but also to the change in kinetic energy of electrons transitioning from bound states to free motion states. For the subsystem of bound electrons, since they do not contribute to pressure, the virial theorem takes the form

$$K_b = -E_b, \tag{13}$$

where index “$b$” indicates that the value refers to bound electrons. Consequently, when an electron leaves an atom and becomes free, its kinetic energy decreases by the binding energy value (ionization potential). Obviously, the excitation of bound electrons also leads to a decrease in the system's kinetic energy. Therefore, the total kinetic energy increment equals

$$dK = d\left(\frac{3}{2}NkT\right) - I_1 dN_e - dE_{exc}, \tag{14}$$

where the last term is the contribution from excited states. Using the relation $N = N_\text{n} + N_\text{e}$, where $N_\text{n}$ is the total number of atoms, after simple transformations we obtain

$$\left(\frac{\partial K}{\partial E}\right)_V = \frac{N_n}{C_V}\left[\frac{3}{2}k\left(1+\alpha\right)\right] - \\ -\frac{N_n}{C_V}\left(I_1 - \frac{3}{2}kT\right)\left(\frac{\partial \alpha}{\partial T}\right)_V - \frac{1}{C_V}\left(\frac{\partial E_{exc}}{\partial T}\right)_V, \tag{15}$$

where $CV = (\partial E/\partial T)_\text{V}$ — the plasma heat capacity, and the degree of ionization is $\alpha = Ne/Nn$. From relation (15), it follows that the derivative $(\partial E/\partial T)_\text{V}$ can become zero and even negative, if the second and third terms combined are greater than the first term.

According to relation (12), the sign of the derivative $(\partial E/\partial T)_\text{V}$ is determined only by the value

of the Grüneisen coefficient. Consequently, the fact that the Grüneisen coefficient values become less than indicates a significant influence of ionization processes and excitation of bound electrons on the thermodynamic properties of plasma. The study of this issue for dense plasma is complicated by difficulties in separating electrons into free and bound ones, as well as accounting for the influence of interactions between plasma particles on their energy spectrum [26].

In this regard, it is interesting to compare the measured dependencies of plasma kinetic energy on the internal energy value with the predictions of CPM. In formula (10), energy is measured from the state where all particles of the system are removed to infinity (and are at rest there). In the experiment, energy is measured from the normal state of a solid. To express kinetic energy through measurable quantities, note that relation (10) should also hold for the state $T = 0$, $P = 0$, for which it takes the form

$$K_0 = -E_0, \tag{16}$$

where the index "0" denotes the state at $T = 0$, $P = 0$. Subtracting equation (16) from (10), we get

$$K - K_0 = 3PV - \left(E - E_0\right). \tag{17}$$

If we neglect the difference between the energy in the normal state and in the state $T = 0$, $P = 0$, then the value $E - E_0$ in the right part of (17) will represent the energy measured in the experiment; below we will continue to denote it with the letter $E$.

Fig. 8 shows a comparison of measured and calculated using CPM dependencies of $K–K_0$ on energy $E$, counted from the normal state. The fact that the kinetic energy of the system remains practically unchanged in the interval $E \leqslant 6$ kJ/g means that the increase in kinetic energy of atoms and free electrons is compensated by the decrease in kinetic energy of bound electrons, which transition to excited bound states or free motion states. The decrease in kinetic energy with increasing internal energy in the interval $E > 6$ kJ/g indicates that here the contribution from ionization and excitation of bound electrons dominates. The large difference between calculated and measured values of plasma kinetic energy indicates that the energy costs for plasma ionization and bound electron excitation in our CPM are greatly underestimated. Therefore, it can be stated that the reason for the discrepancy between model and experimental results lies in insufficiently accurate description of bound states. This fact partly confirms the conclusion about the inadequacy of classical description of non-degenerate dense plasma [27].

Note that the values of the Grüneisen coefficient for metals and silicates at pressures of 10-100 hPa and temperatures $T \leqslant 50$ kK were estimated in shock compression experiments of porous samples [28]. For metals, values of $\gamma = 0.6–0.7$ were obtained, while for silicates, the Grüneisen coefficient turned to zero and even became negative. This anomaly was interpreted by the authors as a consequence of the transition of matter to an amorphous state and partial dissociation of molecules $SiO_2$. Such behavior may also be related to diffuse structural transformations in the liquid state [29].

In conclusion, let's consider the behavior of the resistivity of lead plasma. As is known, one of the theoretically predicted effects of plasma non-ideality is the reduction of ionization potentials. Generally, this effect leads to an increase in the degree of ionization, and with it, the electrical conductivity of plasma, and such an increase in the degree of ionization with increasing density is sometimes called pressure ionization. This effect manifests in the fact that on isotherms, the resistivity decreases with decreasing specific volume. Theoretical models predict the presence of maxima on isotherms of resistivity [14, 23, 30], which separate the region of strongly non-ideal plasma from weakly non-ideal. According to work [23], for lead, the maxima on isotherms of resistivity $T = 10$ kK, $T = 20$ kK are in the volume interval $V/V_0 = 10–20$. The results of our experiments show that in the entire studied region of states for lead plasma, the inequality $(\partial\sigma^{-1}/\partial V)_T > 0$ holds, where $\sigma^{-1}$ – resistivity ($\sigma$ – electrical conductivity). Let's briefly explain where this statement comes from.

First of all, note that as seen in Fig. 2, in the volume interval $V/V_0 = 4–6$ for all presented experiments, the pressure reached its maximum, i.e., in this interval, the heating was close to isobaric and, consequently, the temperature increased with volume increase. In Fig. 7, it can be seen that in this volume interval, the resistivity either increases or remains constant with increasing energy. But since the total derivative of resistivity with respect to volume for

some quasi-static process on the $VT$-plane can be represented as

$$\frac{d\sigma^{-1}}{dV} = \left(\frac{\partial\sigma^{-1}}{\partial T}\right)_V \frac{dT}{dV} + \left(\frac{\partial\sigma^{-1}}{\partial V}\right)_T,$$

and the derivative $(\partial\sigma^{-1}/\partial V)_T < 0$ (as seen in Fig. 7), it follows that $(\partial\sigma^{-1}/\partial V)_T > 0$. For experiments with pressure of 1–2 hPa (see Fig. 2), for which the sample heating process in the volume interval $V/V_0 = 8$–16 was close to isobaric, and the resistivity practically did not change (see Fig. 7), we come to the same conclusion. It can be shown that this is valid for the entire studied region of plasma states, but we won't dwell on this here. Thus, for dense lead plasma studied in this work, "pressure ionization" plays a significant role.

## 5. CONCLUSION

Experimental data on thermodynamic properties and resistivity of dense lead plasma were obtained for a wide range of states on the $VP$-plane. The measurement results were compared with predictions of the chemical model of classical plasma. It was shown that the chemical model underestimates the energy costs for plasma ionization and atom excitation by almost two times. Considerations are provided explaining that the reason for this lies in insufficiently accurate description of bound states. It was shown that measurements of caloric properties of dense plasma together with the use of the virial theorem allows to determine how correctly the theory describes the system's energy division into kinetic and potential. It was also shown that for the dense lead plasma studied here, the "pressure ionization" effect plays a significant role – along isotherms, the resistivity decreases with decreasing specific volume.

## ACKNOWLEDGMENTS

The authors express sincere gratitude to A. S. Shumikhin, who read the manuscript and made several valuable comments.

## REFERENCES

**1.** A. W. DeSilva and A. D. Rakhel, Contrib. Plasma Phys. 45, 236 (2005).

**2.** A. W. DeSilva and G. B. Vunni, Phys. Rev. E 83, 037402 (2011).

**3.** J. Clérouin, P. Noiret, P. Blottiau et al., Phys. Plasmas 19, 082702 (2012).

**4.** P. Renaudin, C. Blancard, J. Clérouin et al., Phys. Rev. Lett. 91, 075002 (2003).

**5.** A. W. DeSilva and A. D. Rakhel, Int. J. Thermophys. 26, 1137 (2005).

**6.** J. Clérouin, P. Noiret, V.N. Korobenko, and A. D. Rakhel, Phys. Rev. B 78, 224203 (2008).

**7.** V. N. Korobenko and A. D. Rakhel, Phys. Rev. B 88, 134203 (2013).

**8.** V. N. Korobenko and A. D. Rakhel, Phys. Rev. B 75, 064208 (2007).

**9.** A. M. Kondratyev, V. N. Korobenko, A. D. Rakhel, J. Exp. Theor. Phys. 127, 1074–1086 (2018)..

**10.** A. M. Kondratyev, V.N. Korobenko, and A. D. Rakhel, J. Phys.: Condens. Matter 19, 195601 (2022).

**11.** L. V. Altshuler, A. V. Bushman, M. V. Zhernokletov et al., JETP 78, 741 (1980) [L. V. Al'tshuler, A. V, Bushman, M. V. Zhernokletov et al., Sov. Phys. JETP 51, 373 (1980)].

**12.** A. D. Rakhel, J. Phys.: Condens. Matter 30, 295602 (2018).

**13.** A. M. Kondratyev and A.D. Rakhel, Phys. Rev. B 107, 195134 (2023).

**14.** E. M. Apfelbaum, Contrib. Plasma Phys. 59, e201800148 (2019).

**15.** E. M. Apfelbaum, Contrib. Plasma Phys. 61, e202100063 (2021).

**16.** A. Yu. Potekhin, G. Chabrier, A. I. Chugunov, E. DeWitt, and F. J. Rogers, Phys. Rev. E 80, 047401 (2009).

**17.** A. L. Khomkin, A. S. Shumikhin, Phys.-Usp. 64, 1125 (1921) [A. L. Khomkin, A. S. Shumikhin, UFN 191, 1187 (2021)].

**18.** V.K. Gryaznov, I. L. Iosilevskiy, and V.E. Fortov, Thermodynamic Properties of Shock- Compressed Plasmas Based on a Chemical Picture, in HighPressure Shock Compression of Solids VII: Shock Waves and Extreme States of Matter, Springer, New York (2004), p. 437.

**19.** R.S. Hixson, M. A. Winkler, and J.W. Shaner, Physica B+ C 139-140, 893 (1986).

**20.** L. D. Landau, E. M. Lifshitz, Theoretical Phy sics: Vol. V. Statistical Physics. Part I. 5th ed. Fizmatlit, Moscow (2002).

**21.** Tables of Physical Values. Reference Book, ed. by I. K. Kikoin. Atomizdat, Moscow (1976).

**22.** L. V. Gurvich, I. V. Veits, V. A. Medvedev et al., Thermodynamic Properties of Individual Substances. Reference Edition in 4 volumes. Nauka, Moscow (1979).

**23.** A. L. Khomkin and A. S. Shumikhin, High Temp. High Press. 49, 143 (2020).

**24.** A. F. Nikiforov, V. G. Novikov, V. B. Uvarov, Quantum-Statistical Models of High- Temperature Plasma and Methods for Calculating Rosseland Mean Free Paths and Equations of State, Fizmatlit, Moscow (2000).

**25.** G. D. Tsakiris and K. Eidmann, J. Quant. Spectr. Rad. Transfer. 38, 353 (1987).

**26.** G. E. Norman, A. N. Starostin, TVT 8, 381 (1970) [G. E. Norman, A. N. Starostin, Teplofiz. Vys. Temp. 6, 410 (1968)]

**27.** G. E. Norman, A. N. Starostin, TVT 6, 410 (1968).

**28.** A. B. Medvedev, R. F. Trunin, UFN 182, 829 (2012).

**29.** V. V. Brazhkin, UFN 182, 847 (2012).

**30.** R. Redmer, Phys. Rep. 282, 35 (1997).